Biomedical Research 2018; 29 (17): 3311-3318 *ISSN 0970-938X*
www.biomedres.info

An experimental model: intrauterine adhesion versus subendometrial fibrosis.

Dina Sabry[1], Abeer Mostafa[1], Dina Mekawey[1*], Zeinab Altaib[2], Ashraf Shamaa[3], Ayman Hany[4], Dalia M. Abd El Hassib[5], Noha E. Ibrahim[6], Warda A. Khalifa[7]

[1]Medical Biochemistry and Molecular Biology, Cairo University, Egypt

[2]Histology and Cell Biology Department, Helwan University, Egypt

[3]Surgery, Anaesthesiology and Radiology Department, Cairo University, Egypt

[4]Gynacology and Obstetric Department, Cairo University, Egypt

[5]Clinical Pathology Department, Benha University, Egypt

[6]Microbial Biotechnology Department,Genetic Engineering and Biotechnology Division,National Research Centre, Giza, Egypt

[7]Biotechnology Department, Sebha University, Libya

Abstract

Background: Intrauterine adhesions (IUA) remain a major cause of infertility. The prevalence of IUA varies geographically and keeps increasing over the last few decades due to increased hysteroscopic surgeries. Therefore, IUA management has received considerable attention. However, the management of IUAs still presents a big challenge: the recurrence rate could be up to 62.5% in severe IUAs. Intrauterine adhesion (IUA) occurs as a result of endometrial destruction by surgical interventions or infection causing obliteration of uterine cavity by the adhesions which interfere with embryonic implantation. Sub endometrial fibrosis may occurs, which causes narrowing of uterine cavity so no enough space for fetal growth. This leads to recurrent abortion.

Aim: We aim in this experiment to apply a method for two models of IUA and or fibrosis by intra-uterine injections of two different doses of trichloroacetic acid.

Method: This experimental study was performed on 30 albino adult rats which were divided into three groups (n=10 rats/group) as follows, group 1: normal control rats, group 2: induced IUA and/or fibrosis that received low dose trichloroacetic acid, group 3: induced fibrosis that received high dose trichloroacetic acid, the extent of fibrosis, vascularization and inflammation were evaluated by; qRT-PCR for IL-6, TNF, VEGF and TG-β immunohistochemistry examination for VEGF and TGF-β and histological assessment.

Results: We found significant increase in IL-6, TNF and TGF in high dose group and significant decrease in VEGF in high dose group compared to normal group and low dose group ($p<0.05$).

Discussion: The reproductive cells are the most sensitive to toxic environmental materials. In this study, we found that group II rats (IUAs), unlike control rats, had impaired endometrial epithelial cells, a lower number of endometrial glands, higher inflammatory cell infiltration, poor vascularity, and a severe narrowing of the uterine cavity with dense endometrial fibrosis as confirmed by H&E and Masson's trichrome staining.

Keywords: IUA, Sub endometrial fibrosis, IL-6, TNF, VEGF, TGF-β.

Abbreviations:

IUA: Intrauterine Adhesion TGF-β; Transforming Growth Factor-β; VEGF: Vascular Endothelial Growth Factor; EMT: Epithelial-Mesenchymal Transition; TNF: Tumor Necrosis Factor; IL-1: Interleukin 1; IL-6: Interleukin 6; IL-10: Interleukin 10; H&E: Hematoxylin and Eosin; CT: Critical Threshold; ECM: Extracellular Matrix.

Accepted on September 10, 2018

Introduction

Intrauterine adhesion (IUA), which is caused by damage to the endometrial reached to basement membrane and exposure of myometrial tissue, is a common gynecological disease that is also referred to as Asherman's syndrome [1]. Uterine synechia or IUA, is a partial or complete obliteration of the uterine cavity and/or the cervical canal. Which cause menstrual abnormalities, infertility and recurrent pregnancy miscarriage. Synechia can occur as a consequence of uterine surgery. It essentially occurs after a uterine curettage, performed in cases of miscarriage, pregnancy termination or evacuation of placental products in the postpartum period or hysteroscopic surgery, including myomectomy, polypectomy and endometrial ablation. Synechia may also occur after a cesarean section or a uterine devascularization in cases of severe postpartum hemorrhage [2]. Infections particularly tuberculosis which has been shown to induce severe damage is also recognized as a cause of intrauterine adhesions [3]. The fibrosis is progressive and chronic process. It results from interaction of inflammatory cytokines such as IL-6, TNF and fibrotic factors as TGF. This interaction allows excessive accumulation of the extracellular matrix (ECM), which is a key step in fibrosis [4].

Material and Methods

Experimental animals

Thirty adult female Albino rats (180-220 g) weight, 6 w of age, have been beard before were obtained from the Animal House of Faculty of Medicine; Cairo University were included in this study. The animals were housed in wire mesh cages at room temperature with 12:12 h light-dark cycles and were maintained on standard rat chow and tap water. Veterinary care was provided by the Animal House Unit of Cairo University. An approval from Institutional Review Board and Institutional Animal Care and Use Committee was taken prior to starting study. The rats were cycle synchronized according to a vaginal smear analysis which allows for the determination of the phases of the 4 d estrus cycle: proestrus, estrus, metestrus, and diestrus. The animals were randomly divided into 3 groups of 10 animals for each; group 1: ten rats as a control group (non-injected rat). Group 2: Low dose group includes ten rats injected 0.1 ml of trichloroacetic acid 2% conc into right uterine horn. Group 3: high dose group includes ten rats injected 0.1 ml of trichloroacetic acid 10% conc into right uterine horn [5]. The last two groups were applied for induction of IUA and/or endometrial fibrosis as follows; anesthesia was induced by Flutothane inhalation then the abdomen was shaved and then draped in a sterile way. The uterine horns were exposed by an abdominal midline vertical incision and a piece of gauze was used to wrap right uterine horn to prevent abdominal viscera. The pelvic region was examined to exclude any adhesions or macroscopic abnormality. 0.1 ml of trichloroacetic acid was injected into right uterine horn but left horn was set as control. The uteri were gently returned to their pelvic location without disrupting. At the end of 4 w after surgical intervention all rats after overnight fasting were sacrificed [5] and bilateral uterine horns were dissected the uterus was removed and uterine horns fixed overnight in 4% parformaldehyde at 4°C and subjected to histological, immunohistochemical evaluations and molecular study.

Histological evaluation

The uterine horns were cut, by serial small transverse sections and put into processing cassette. Then, the paraffin blocks were prepared from each cassette separately. Specimens were washed under running tap water for 24 h and dehydrated with ascending concentrations of ethanol with 50, 70, 90, and 3 changes of 100%. The specimens were then put in a 1:1 ratio of xylene and absolute alcohol for 1 h, followed by three changes of xylene overnight, for transparency. Then, the specimens were made into paraffin blocks using a 1:1 xylol and paraffin mixture for 1 h and paraffin for 6 h in an incubator. Briefly, 4-6 μm thick sections were obtained using a microtome, mounted on glass slides and dried at 60°C for 30 min. All slides were de-paraffinized using xylene and then rehydrated in decreasing concentrations of ethanol and stained with Hematoxylene and Eosin (H&E) (According to application procedure of Bio Optica Milano, ITALY), rehydrated, and mounted as described previously for general structure examination, Masson's trichrome stain (for high lighting fibrosis) and an immunohistochemical evaluation of vascular endothelial growth factor (VEGF) (a vascular marker) and transforming growth factor (TGF)-β (a fibrotic marker) were also performed [6].

Immunhistochemical evaluation

After slides prepared and de-paraffinzed as discussed before, Antigen retrieval was performed using microwave heating (three times of 10 min; antigen retrieval was performed using microwave heating, 10 mM citrate buffer, pH6.0) after inhibition of endogenous peroxidase for 15 min). The slides were incubated for 1 h with rabbit polyclonal antibodies to VEGF (1:100 Thermo scientific, USA), VEGF antibody (VG1) Novus Biologicals (NB100-664)), TGF-β antibody) Santa Cruz (Cat #sc-130348) at room temperature, then washed using PBS and then incubated with secondary antibody (Invitrogen, UK) for 15 min followed by PBS wash. Finally, the detection of bound antibody was accomplished using the avidin biotin complex (ABC) reagent for 20 min then PBS wash. A 0.1 % solution of diaminobenzidine (DAB) (DAB, thermo scientific, USA) was used for 5 min as a chromogen. Slides were counterstained with Mayer's hematoxylin for 5-10 min. dehydrated, and mounted as described previously [7]. Then histological examinations were performed under a magnification of 200X to evaluate immune positive expression for VEGF and TGF-β and averaged from at least 5 randomly selected fields.

Morphometric study

The mean area percentage of VEGF expression and TGF-β were quantified for five images from five non-overlapping

fields from each rat of each group using the Image-Pro Plus program version 6.0 (Media Cybernetics Inc, Bethesda, Maryland, USA).

Quantitative RT-PCR

Real time PCR was performed for quantitative genes expression of interleukin 6 (IL-6), tumor necrosis factor-α (TNF-α), vascular endothelial growth factor (VEGF) and transforming growth factor-β (TGF-β). Uterine samples of all studied groups were lysed and total RNA was isolated with Thermo Fisher Scientific Inc. Germany. (Gene JET, Kit, #K0732).Ten ng of the total RNA from each sample were used for reverse transcription with subsequent amplification with Bioline, a median life science company, UK (SensiFAST™ SYBR® Hi-ROX) one-Step Kit (catalog no. PI-50217 V) in a 48-well plate using the Step One instrument (Applied Biosystem, USA). Thermal profile was as follows: 45°C for 15 min one cycle (for cDNA synthesis), 10 min at 95ºC for reverse transcriptase enzyme inactivation followed by 40 cycles PCR amplification. Each cycle was 10 s at 95°C, 30 s at 60°C and 30 s at 72°C. Changes in the expression of each target gene were normalized relative to the mean critical threshold (CT) values of GAPDH as housekeeping gene by the $\Delta\Delta C_t$ method. Primers sequence for all studied genes was demonstrated in Table 1.

Western blot

The IL-6, TNF, TGF-β, VEGF and β-actin antibodies used were purchased from Thermo Scientific (MA1-26771). Proteins were extracted from uterine tissue by RIPA lysis buffer which were provided by Bio Basic Inc. (Markham, Ontario L3R 8T4, Canada). Extracted proteins were separated by SDS/PAGE on 4-20% polyacrylamide gradient gels. After incubation in 5% non-fat dry milk, tris/HCl, 0.1% tween 20 for 1 h; IL-6, TNF, TGF-β, VEGF and β-actin monoclonal antibodies were added to one of the membranes containing specimen samples and incubated at 4°C overnight. Appropriate secondary antibodies were incubated for 2 h at room temperature. After being washed twice with 1X TBST, densitometric analyses of the immunoblots were performed to quantitate the amount of IL-6, TNF, TGF-β, VEGF against control sample by total protein normalization using image analysis software on the ChemiDocMP imaging system (version 3) produced by Bio-Rad (Hercules, CA).

Statistical analysis

Data were coded and entered using the statistical package SPSS version 22. Data was summarized using mean and standard deviation. Comparisons between groups were done using analysis of variance (ANOVA) with multiple comparisons post hoc test [8]. P-values less than 0.05 were considered as statistically significant. Data were expressed as mean ± SD, p value<0.05 was significant.*statistically significant compared to corresponding value in normal control group. #statistically significant compared to corresponding value in low dose group.

Results

Histological results

1-hematoxylin and eosin (H&E) stained sections: Examinations of the sections of rat's uteri of all groups by low and high power showed:

In group I (control group): Normal architecture of the uterine histology was composed of three layers endometrium, myometrium, and perimetrium. The inner endometrium presented with intact extensive folded and had a patent wide irregular uterine lumen contained little secretion. The endometrium was lined by simple columnar partially ciliated epithelium with basally located oval or rounded nuclei and underlying connective tissue stroma surrounding numerous rounded or oval uterine glands. At some areas stroma cycled around two glands in the form of eight figures around them. Some of the glands were contained secretions in their lumen and tiny blood vessels could be observed. The thick middle layer of myometrium constituted by layers of well-organized smooth muscles and outer perimetrium presented histological pattern of squamous epithelium sustained on the dense connective tissue could be detected. The few of mitotic figures were also observed in both epithelial cells lining uterine cavity and uterine glands (Figures 1A-1D).

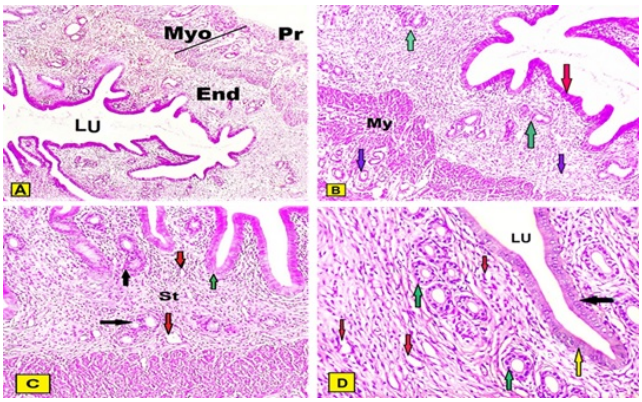

Figure 1. *Photomicrographs of a sections of a rat uterus in group 1 (control) stained with H&E showing: A: The normal uterine architecture presented with intact endothelium and patent wide uterine Lumen (UL) with different layers; endometrium (End), myometrium (myo) with normal thickness (line), and perimetrium (pr) (X40). B: The uterine cavity was widely open contain secretion. The intact endometrium with normal epithelial lining and numerous mucosal folds (red arrow). Stroma containing numerous uterine glands (green arrow) and tiny blood vessels (blue arrows) (X100). C: The intact endometrium with normal thickness of endometrial layer (green arrow) lined by simple high columnar partially ciliated epithelium with basally located oval nuclei and underlying compact highly cellular connective tissue stroma (St) surrounding uterine glands, forming eight figures (black arrows) at some areas, some of the glands are seen filled with secretions and numerous tiny blood vessels (yellow arrows) are detected (X200). D: Endometrium with part of lumen intact epithelium (black arrows), and mitotic figures was observed (yellow arrows).Round and oval uterine glands with intact columnar epithelium (green arrow) and numerous tiny blood vessels (red arrows) are detected.*

In group II (low dose trichloroacetic acid intrauterine injection): The studied sections of rats uteri showed: Narrowing of uterine lumen of the injected right horn, abnormal architecture of the three layers, marked increased thickness of the endometrium, decreased in the myometrium and perimetrium. Some of them showed narrowing of uterine lumen and absence of mucosal folds. The intact lining epithelium was simple low cubical, but the detached epithelium from focal areas was observed. Few of glands and few and dilated blood vessels under the epithelial layer were presented. Some of them showed moderate endometrial infiltration of Polymorphonuclear cells. Their thick stroma was observed cycling around few of glands forming eight Figures. Also, proliferative changes in adjacent or remote areas to these degenerative patches with increased number of strata. Although numbers of layers increased, the epithelium appeared riddled and many cells in different strata, even the basal ones, showed areas of degeneration and vacuolations with numerous pyknotic nuclei (Figure 2A-2D).

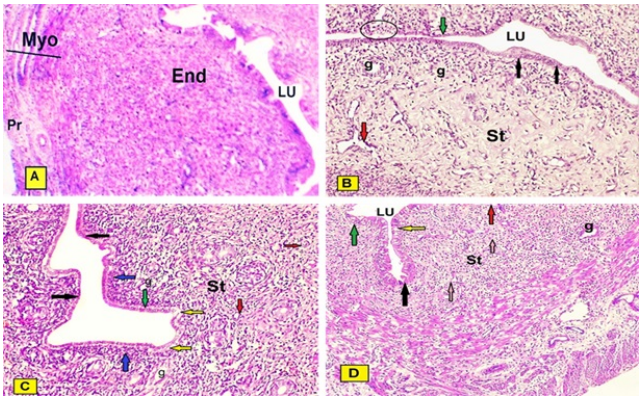

Figure 2. *Photomicrographs of a sections of a rat uterus in group II (low dose trichloroacetic acid) stained with H&E showing: A: Narrow of uterine lumen (LU) of the injected right horn, abnormal architecture, thick endometrium (End) marked in its stroma, decrease in the thickness of the myometrium (line) and perimetrium (Pr) (X40). B: Narrowing of uterine lumen (Lu) and absence of mucosal folds. The endometrial surface is lined by low cubical (black arrow) area of partially detached epithelium (green arrow) of epithelial lining. Few of glands (g) and few of dialated blood vessels (red arrow) (X200). C: Polymorph nuclear cells infiltration (blue arrow), and around the endometrial glands and dilated congested blood vessels (blue arrow). The uterine glands have narrow irregular lumen and flat lining epithelium (green arrows). The lamina propria (blue arrow) (X200). D: Narrow uterine lumen (Lu) lined by low columnar epithelium (green arrow) some of cells are vacuolated (yellow arrow), their nuclei showing pyknosis area of separated cells. Also few and small endometrial glands (g), tiny and few blood vessels red arrow could be seen (X200).*

In group III (High dose of trichloroacetic acid intrauterine injections of the right horn) showed: Very narrow of uterine lumen of the injected right horn which showed areas of complete epithelial adhesion, abnormal architecture in the three layers, the epithelial lining decreased in the thickness, but subenothelial layer were markedly increased. The myometrium and perimetrium were decreased. Some areas of endometrium were appeared bared from epithelial cell lining and absence of mucosal folds, with few small glands under the epithelial layer. Also dilated congested blood vessel and areas of polymorphonuclear cells infiltrating the lamina propria are also observed. Also, in small blood vessels marked decreased of uterine glands were observed and their lining epithelium was cubical and had vaculated cytoplasm. Thick compacted stroma could be detected (Figures 3A-3D).

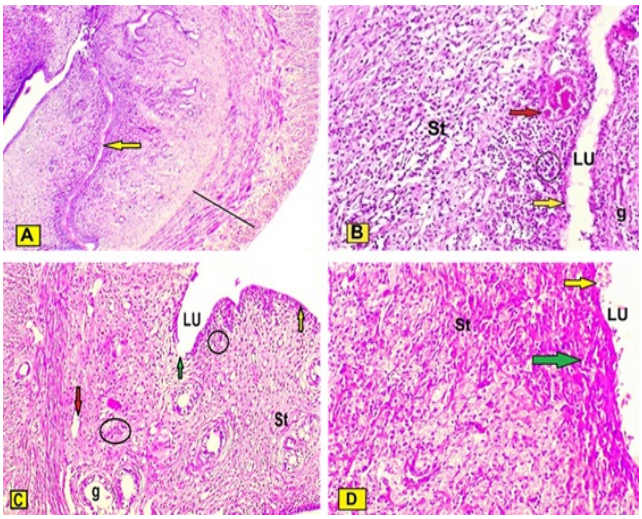

Figure 3. *Photomicrographs of a sections of the right horn of the rats uteri in group III (High dose of trichloroacetic acid) stained with H&E showing: A: Very narrow of uterine lumen (LU) of the injected right horn which show areas of complete adhesion (yellow arrow), abnormal architecture in the three layers endometrium (End), decrease in the thickness of the myometrium (line) and perimetrium (Pr) (X40). B: Narrowing of uterine lumen (Lu), its endometrium is bared from epithelial cell lining (yellow arrow) and absence of mucosal folds , with few small glands(g) under the epithelial layer also dialated congested blood vessel (red arrow) and areas of polymorphonuclear cells (circle) infiltrating the lamina propria are also observed (X200). C: Part of uterine lumen (lu) and its lining showing bare area from epithelium (green arrow) and area of flat lining epithelium (yellow arrows). Under the epithelium polymorphonuclear cells infiltration (circle) and there are small blood vessels (red arrow). Few of uterine glands (g) cubical epithelial lining which have vaculated cytoplasm and their thick stroma and forming 8 figures around few of glands (X200). D: Part of endometium bared from (yellow arrow) and absence of mucosal folds (arrow). Thick compacted stroma (st) could be detected (X200).*

Masson's trichrome stain: A studied sections in rats uteri of all groups are stained with Masson trichrome (X200) showed:

In group 1 (control): The stroma had almost a few of collagen fiber deposition (Figure 4A).

In group II (low dose injection): There was loose increase in collagen fibers deposition are detected under epithelium, in the stroma surrounding the glands and blood vessels compared with the control group (Figures 4B1and 4B2).

In group III (high dose injection): Revealed a moderate increase in the collagen fibers deposition under the endometrium, in the stroma surrounding uterine glands and blood vessels, compared with group II (Figure 4C).

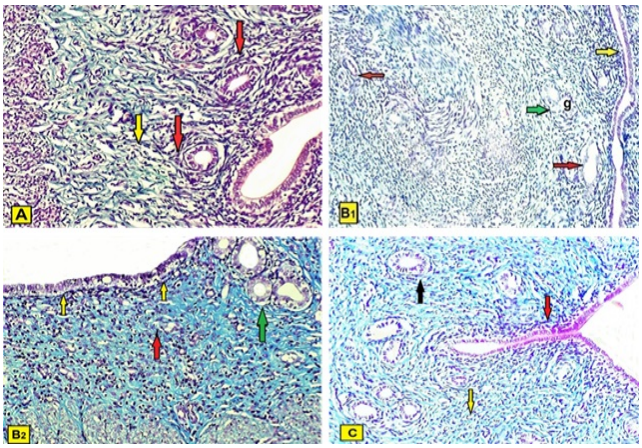

Figure 4. Photomicrographs of a section in rats uteri of all groups are stained with Masson trichrome (X200) A: In group 1 (control) showing the endometrial stroma had almost a few of collagen fiber deposition B: In group II (low dose injection). There were increase in collagen fibers deposition are detected under epithelium (yellow arrows) in the stroma surrounding blood vessels (yellow arrows) and connective tissue stroma surrounding glands (yellow arrows) (B1 and B2) compared with that in the control group (B1 and B2). C: In group III (high dose) revealed a marked increase in the collagen fibers deposition under the endometrium (red arrow) in the stroma surrounding blood vessels (yellow arrows) and surrounding glands (black arrows), compared with that in group II.

Immunohistochemical results: a. VEGF immune expression. In all groups (XC200) showed:

The positive reactions were assessed by the presence of brown nuclei (Figures 5A-5C).

In group I (Control group): Negative reaction in epithelial cells of the endometrium, in uterine glands, stroma and blood vessels (Figure 5A).

In group II (low does): Positive reaction epithelial cells of the endometrium, in uterine glands, blood vessels and stroma (Figure 5B).

In group III (High dose): Positive reaction in epithelial cells of the endometrium, in uterine glands, blood vessels and stroma (Figure 5C).

b. TGF-β immune expression. In all groups (X200) showed: To assess the extent of IUA, we evaluated TGF-β immune expression since TGF-β plays an important role in fibrosis formation. TGF-β was mainly expressed in the nucleus and in the cytoplasm of stromal and epithelial cells.

In group1 (control): Negative reaction in epithelial cells of the endometrium, in uterine glands, blood vessels and stroma (Figure 6A).

In group II (Low dose): Positive reaction of endometrium epithelial cells in uterine glands and stroma and blood vessels (Figure 6B).

In group III (High dose): Positive reaction in endometrium epithelial cells, in the uterine glands, blood vessels and stroma (Figures 6C1 and 6C2).

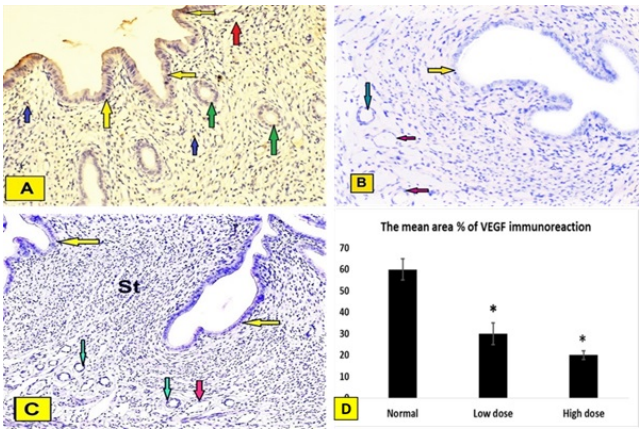

Figure 5. Photomicrographs of the sections of rats uteri immuno-stained with VEGF (X200) showing: A: In group 1 (control): positive reaction in endometrium epithelial cells (yellow arrow), in uterine glands (green arrow), blood vessels (red arrow) and stroma (blue arrow). B: In group II (low dose): negative reaction of endometrium epithelial cells (yellow arrow), in uterine glands (green arrow), blood vessels (red arrow) and stroma (st). C: In group III (High dose): negative reaction in endometrial epithelial cells (yellow arrow), in uterine glands (green arrow), blood vessels (red arrow) and stroma (St).

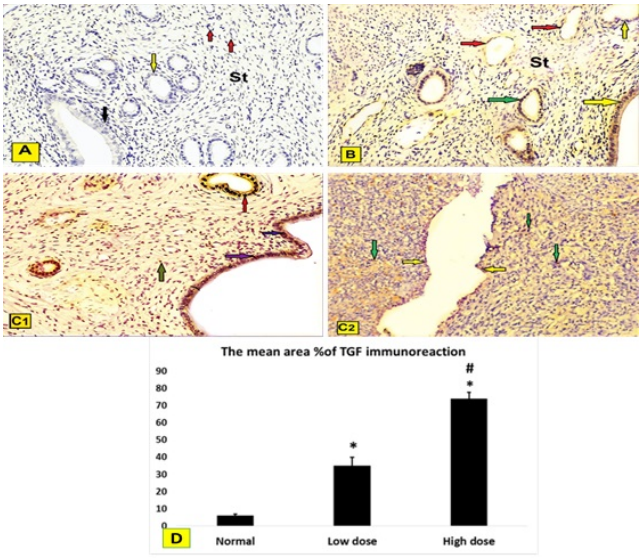

Figure 6. Photomicrographs of sections of rats uteri in all groups showing expression of TGF-β (X200) showing: A: In group1 (control): negative reaction in endometrium epithelial cells (black arrow), in uterine glands (yellow arrow), blood vessels (red arrow) and stroma (st). B: In group II (Low dose) positive reaction of endometrium epithelial cells (yellow arrow), in uterine glands (green arrow) and stroma (st) and blood vessels (red arrow). C1: In group III (High dose): positive reaction in endometrium epithelial cells (yellow arrow), in uterine glands (green arrow), blood vessels (red arrow). C2 positive reaction in endometrium (yellow arrow), and stroma (green arrow) blood vessels (red arrow).

Statistical analysis

Immunhistochemical staining of VEGF was assessed by the presence of brown nuclear positive reactivity, staining index was decreased in uterine tissue of both low dose and high dose

groups compared to normal control group (Figure 5D). TGF was assessed by the presence of brown nuclear and cytoplasm positive reactivity, staining index was increased in uterine tissue of both low dose and high dose groups compared to normal control group with significant increase in high dose group when compared to low dose group (Figure 6D).

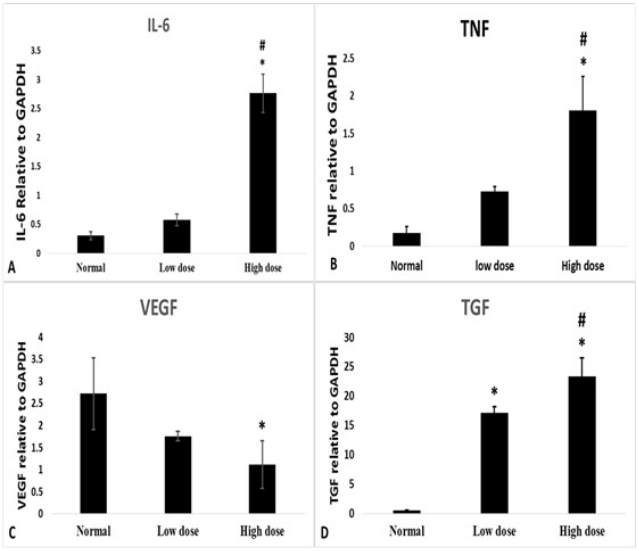

Figure 7. Quantitative genes expression of the target genes in all studied groups A: IL-6, B: TNF, C: VEGF, D: TGF-β.

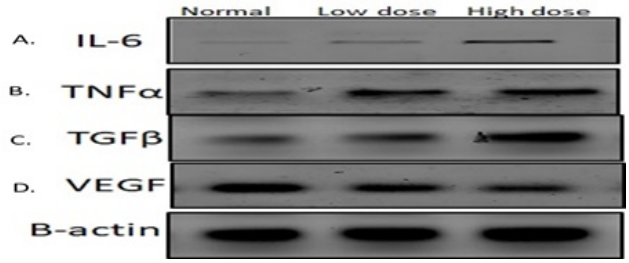

Figure 8. The quantitative scanning densitometry results of IL-6, TNF, TGF-β, and VEGF normalized compared with β-actin protein levels in all groups.

PCR gene expression results

Inflammatory cytokines (IL-6) showed statistical significant increase in high dose group compared to normal control group (p=0.000) and low dose group (p=0.000) (Figure 7A), also TNF gene expression showed statistical significant increase in high dose groups compared to normal control group (p=0.002) and low dose group (P=0.016) (Figure 7B). VEGF expression level has a statistical significant decrease in high dose groups compared to normal control group (p=0.03) (Figure 7C).

As regard the fibrotic marker (TGF-β), there was a statistical significant increase in both low dose and high dose groups compared to normal control group (p=0.000) and more significant increase in high dose groups compared to low dose group (p=0.000) (Figure 7D).

Western blot results

Inflammatory cytokines (IL-6) showed statistical significant increase in its expression in low and high dose groups compared to normal control group (p=0.000) and statistical significant increase in its expression in high dose group compared to low dose group (p=0.000) (Figures 8 and 9A), also TNF protein level showed statistical significant increase in its expression in low and high dose groups compared to normal control group (p=0.001, 0.00) respectively, and statistical significant increase in its expression in high dose group compared to low dose group (P=0.001) (Figures 8 and 9B). As regard the fibrotic marker (TGF-β), there was a statistical significant increase in both low dose and high dose groups compared to normal control group (p=0.004, 0.000) respectively and significant increase in high dose groups compared to low dose group (p=0.001) (Figures 8 and 9C). VEGF protein level has a statistical significant decrease in its expression in low and high dose groups compared to normal control group (p=0.000) and significant decrease in high dose groups compared to low dose group (p=0.01) (Figures 8 and 9D).

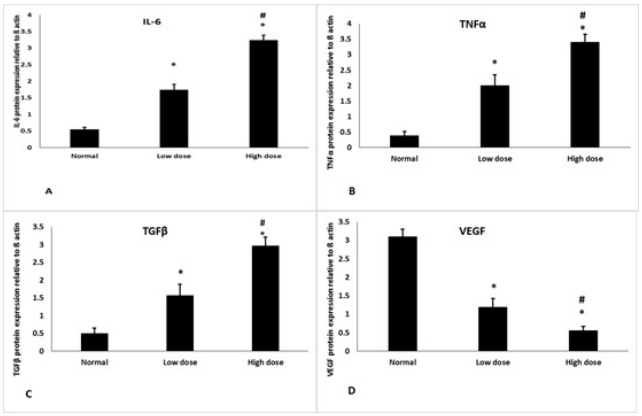

Figure 9. Western blot analysis showing IL-6, TNF, TGF-β, VEGF relative to β-actin proteins in all studied groups.

Table 1. Primers sequence of all studied genes.

Gene	Primer sequence from 5'- 3'	Gene bank accession number
TGF-β	Forward: CTACTGCTTCAGCTCCACAG	
	Reverse: GCACTTGCAGGAGCGCAC	XM016135677.1
TNF-α	Forward: GCCTCTTCTCATTCCTGCTT	AF269160.1
	Reverse: CACTTGGTGGTTTGCTACGA	
VEGF	Forward: CTCCGAAACCATGAACTTTCTGCTC	
	Reverse: CAGCCTGGCTCACCGCCTTGGCTT	NM031836.2
IL6	Forward: TTCCATCCAGTTGCCTTCTT	NM001314054.1
	Reverse: ATTTCCACGATTTCCCAGAG	
GAPDH	Forward: ACAGTCCATGCCATCACTGCC	NG009348.3

Reverse: GCCTGCTTCACCACCTTCTTG

Discussion

The reproductive cells are the most sensitive to toxic environmental materials.

In this study, we found that group II rats (IUAs), unlike control rats, had impaired endometrial epithelial cells, a lower number of endometrial glands, higher inflammatory cell infiltration, poor vascularity, and a severe narrowing of the uterine cavity with dense endometrial fibrosis as confirmed by H&E and Masson's trichrome staining. These results agreed with the results of Sabry et al. [5], who revealed dense fibrosis, severe inflammation, a necrotic endothelium. Uterine fibrosis either IUA or subendometrial fibrosis occurs as a result of interaction between inflammatory and fibrotic cytokines.IL-6 acts as a pro-inflammatory cytokine that is secreted by T cells and macrophages and stimulates immune response [9]. IL-6 contributes to the development of fibrosis by modulating TGF-β signaling and stimulating the proliferation of fibroblasts, as well as the collagen production [10]. In our previous study [5], we found significant increase in *IL6*, *TNF*, *TGF* genes expression and significant decrease in *VEGF* gene expression in endometrial fibrosis group compared to normal group. The current results revealed that a significant increase in high dose groups compared to normal control group and low dose group. This agreed with a mare model of endometritis by doing cervical occlusion after artificial insemination. The expression of IL-1, IL-6, IL-10 and TNF were analysed by Western blotting, and found significant increase in their levels compared to the control group [11].

Tumor necrosis factor (TNF) is a cell signaling protein involved in systemic inflammation and is one of the cytokines that make up the acute phase reaction. It is produced chiefly by activated macrophages, although it can be produced by many other cell types such as $CD4^+$ lymphocytes, natural killer cells, neutrophils, mast cells, and eosinophils [12]. TNF induces the fibrosis by up-regulating collagen accumulation; moreover, it has mitogenic effects in myofibroblasts and is able to extend the inflammatory state thus increasing the expression of other inflammation mediators, such as IL-6 and IL-1, and activating NFκB-dependent pathways, a transcription factor that increases the expression of cytokines, enzymes and adhesion molecules [13]. The current results revealed that a significant increase in high dose groups compared to normal control group and low dose group.

The current results supported by a model of pulmonary fibrosis. Inflammation was assessed by measuring the levels of TNF, IL-1β and IL-6 in broncho-alveolar lavage fluid, they found that these inflammatory cytokines were increased in fibrosis group compared to normal group [14].

Vascular endothelial growth factor (VEGF) is a signal protein produced by cells that stimulate vasculogenesis and angiogenesis. It is part of the system that restores the oxygen supply to tissues when blood circulation is inadequate such as in hypoxic conditions [15]. The current results revealed that VEGF expression level has a statistical significant decrease high dose groups compared to normal control group, this agreed with a\study on 36 patients with severe intrauterine adhesions; who were subjected to trans-cervical resection of adhesions by hysteroscopy and reported vascular closure and hypoxic changes in the endometrial tissues of these patients [16], also agreed with another study which revealed significant decrease in VEGF staining in Asherman rat group [17].

Transforming growth factor-beta (TGF-β) is an important cytokine for the induction of the epithelial-mesenchymal transition (EMT) in fibrosis. TGF-β signaling induces the EMT through various signaling mechanisms and is the predominant agent mediating these fibrotic changes. Chronic exposure to TGF-β induces the transition of normal cells to collagen-producing mesenchymal cells; thus increases the expression of collagen and induces cytoskeletal rearrangement that resembles the EMT [18].

The present study revealed significant increase in both low dose and high dose groups compared to normal control group and more significant increase in high dose groups compared to low dose group. The concentration of TGF-β increased after uterine surgery. The concentration of TGF-β in the IUA patient was significantly higher than normal females. Also the concentration of TGF-β was positively associated with area of intrauterine adhesion. So TGF-β cytokines might be involved in reformation of intrauterine adhesions [19]. Also in a model of uterine adenomyosis the immunohistochemistry staining was performed in endometrial tissue to quantify the extent of fibrosis in lesions. TGF-β immune reactivity was high in adenomyosis group compared to its level in normal control group [20]. The serum TGF-β level of patient with uterine fibroid was significantly higher than that of healthy subjects [21].

Conclusion

From the present study, we can conclude that serious injuries to the endometrium in fertility age can often cause intra-uterine adhesion (IUA), thin endometrium or subendometrial fibrosis depending on the degree of injury, all of them interfere with the fertility. However, the complex nature of the uterine environment and function limits the possibilities of effective treatment. Therefore, it is an urgent gynecological need to explore novel treatment methods to repair endometrial damage, improve its microenvironment and tolerance status, and enhance the pregnancy rate in infertile patients.

References

1. Yu D, Wong YM, Cheong Y, Xia E, Li TC. Asherman syndrome-one century later. Fertil Steril 2008; 89: 759-779.
2. Bazoobandi S, Tanideh N, Rahmanifar F, Tamadon A, Keshtkar M, Mehrabani D, Kasraeian M, Koohi-Hosseinabadi O. Induction of Ashermans Syndrome in rabbit. J Reprod Infertil 2016; 17: 10-16.

3. Mohamed K, Olivier M, Ali H, Pascale C, Herve F. Evaluation of the rabbit as an experimental model for human uterine synechia. J Human Reprod Sci 2012; 5: 175-180.
4. Speca S, Giusti I, Rieder F, Latella G. Cellular and molecular mechanisms of intestinal fibrosis. World J Gastroenterol 2012; 18: 3635-3661.
5. Sabry D, Mostafa A, MarzoukS, Ibrahim W, Ali HHM, Hassan A and Shamaa A. Neupogen and mesenchymal stem cells are the novel therapeutic agents in regeneration of induced endometrial fibrosis in experimental rats. Biosci Rep 2017; 11; 37: 20170794.
6. Suvarna KS, Layton C, Bancroft JD. Bancrofts theory and practice of histological techniques E-book. Elsevier Health Sciences 2018.
7. Li J, Cen B, Chen S, He Y. MicroRNA-29b inhibits TGF-β1-induced fibrosis via regulation of the TGF-β1/Smad pathway in primary human endometrial stromal cells. Mol Med Rep 2016; 13: 4229-4237.
8. Chan YH. Biostatistics 102: quantitative data-parametric & non-parametric tests. Singapore Med J 2003; 44: 391-396.
9. Kobayashi T, Tanaka K, Fujita T, Umezawa H, Amano H, Yoshioka K, Naito Y, Hatano M, Kimura S, Tatsumi K, Kasuya Y. Bidirectional role of IL-6 signal in pathogenesis of lung fibrosis. Respir Res 2015; 16: 99.
10. Diaz JA, Booth AJ, Lu G, Wood SC, Pinsky DJ, Bishop DK. Critical role for IL-6 in hypertrophy and fibrosis in chronic cardiac allograft rejection. Am J Transplant 2009; 9: 1773-1783.
11. Reilas T, Rivera M, Liepina E, Yeste M, Katila T. Effects on the equine endometrium of cervical occlusion after insemination. Theriogenology 2016; 85: 617-624.
12. Cheslack K, Cremers S, Bao Y, Shen L, Schaefer C, Brown A. Maternal serum cytokine levels and risk of bipolar disorder. Brain Behav Immun 2016; 1591: 30353-30361.
13. Sands BE, Kaplan GG. The role of TNFalpha in ulcerative colitis. J Clin Pharmacol 2007; 47: 930-941.
14. Yu W, Sun L, Yang H. Inhibitory effects of astragaloside IV on bleomycin-induced pulmonary fibrosis in rats via attenuation of oxidative stress and inflammation. Inflammation 2016.
15. Weinkopff T, Konradt C, Christian D, Discher D, Hunter C, Scott P. Leishmania major infection-induced VEGF-A/VEGFR-2 signaling promotes lymphangiogenesis that controls disease. J Immunol 2016; 197: 1823-1831.
16. Chen Y, Chang Y, Yao S. Role of angiogenesis in endometrial repair of patients with severe intrauterine adhesion. Int J Clin Exp Pathol 2013; 6: 1343-1345.
17. Kilic S, Yuksel, Pinarli F, Albayrak A, Boztok B, Delibasi T. Effect of stem cell application on Ashermansyndrome,an experimental rat model. J Assist Reprod Gene 2014; 31: 975-982.
18. Bi W, Yang C, Shi Q. Transforming growth factor-ß1 induced epithelial-msenchymal transition in hepatic fibrosis. Hepatogastroenterology 2012; 59: 1960-1963.
19. Tao Z, Duan H. Expression of adhesion-related cytokines in the uterine fluid after transcervical resection of adhesion. Chinese J Obstetr Gynecol 2012; 47: 734-737.
20. Shen M, Liu X, Zhang H, Guo S. Transforming growth factor β1 signaling coincides with epithelial mesenchymal transition and fibroblast to myofibroblast trans-differentiation in the development of adenomyosis in mice. Hum Reprod 2016; 31: 355-369.
21. Shen T, Shi H, Xu Q, Song Q, Xu Y, Huang Y. Effects of TGF-β on uterine fibroids of women of childbearing age and uterine artery embolization. Minim Invasive Ther Allied Technol 2017; 26: 292-299.

*Correspondence to

Dina Mekawey

Medical Biochemistry and Molecular Biology

Cairo University

Egypt